Wasit Journal for Pure Science

Journal Homepage: https://wjps.uowasit.edu.iq/index.php/wjps/index
e-ISSN: 2790-5241 p-ISSN: 2790-5233

Green Synthesis of Silver Nitrate Nanoparticles from E. coli and Evaluation of Their Inhibitory Effectiveness against *E. coli, S. aureus, and B. subtilis*

Dheyaa Abdulhussein Mohsin[1]*, Hashim Ali Yusr [2]

[1,2]College of Science, University of Waist, Waist, IRAQ

*Corresponding Author: Dheyaa Abdulhussein Mohsin

DOI: https://doi.org/ 10.31185/wjps.389
Received 10 April 2024; Accepted 04 Jun 2024; Available online 30 Jun 2024

ABSTRACT: This study investigates the environmentally friendly production of silver nitrate nanoparticles (AgNPs) utilizing Escherichia coli (E. coli) and assesses their ability to kill harmful bacteria such as E. coli, Staphylococcus aureus, and Bacillus subtilis. Employing biological processes for nanoparticle synthesis offers both ecological advantages and improved compatibility with biological systems. The biogenic synthesis process entailed cultivating E. coli in Tryptic Soy Broth, and subsequently treating it with a silver nitrate solution to generate AgNPs. The produced nanoparticles underwent characterization using Scanning Electron Microscopy (SEM), X-Ray Diffraction (XRD), and Energy-Dispersive X-ray (EDX) examination. The antibacterial efficacy was evaluated by quantifying the zones of inhibition against the microorganisms being tested, indicating that higher quantities of AgNPs were associated with greater antibacterial potency. This study emphasizes the possibility of utilizing biologically produced nanoparticles in medical applications, namely as a substitute for conventional antibacterial treatments, which frequently encounter challenges related to resistance.

Keywords: Green synthesis, silver nanoparticles, X-ray diffraction, scanning electron microscopy.

1. INTRODUCTION

In the rapidly growing field of nanotechnology, the production of metal nanoparticles has established a specialized position, especially in the medicine and the environment [1, 4]. Silver has attracted significant attention among other metals because of its notable antibacterial characteristics, resulting in extensive research on its potential uses [2, 3]. Conventional techniques for producing silver nanoparticles typically employ chemical and physical procedures that frequently use harmful solvents and produce dangerous waste products. Although these approaches are successful, they also present substantial environmental and health hazards, emphasizing the importance of adopting more sustainable practices [5].

To solve these difficulties, the green synthesis of nanoparticles has become a favorable option, providing a more ecologically friendly and cost-efficient method. This approach employs biological organisms such as bacteria, fungi, and plants, reducing the negative effects on the environment and improving the compatibility of the nanoparticles with living systems. The use of Escherichia coli for the synthesis of silver nanoparticles provides a unique approach to exploiting microbial pathways for nanoparticle creation. The biogenic pathway not only increases sustainability, but it also allows nanoparticles to be modified in a way that has the potential to suppress microbial growth [6, 7, and 8]. This study investigates a novel, efficient, and environmentally friendly technique for producing silver nitrate nanoparticles by utilizing the bacterium Escherichia coli in a single step. By harnessing the inherent mechanisms of this microbe, our objective is to generate nanoparticles that are not only less detrimental to manufacture but also more potent in combating

pathogenic bacteria. The synthesized nanoparticles were assessed for their antibacterial effectiveness against important bacterial pathogens, specifically Escherichia coli, Staphylococcus aureus, and Bacillus subtilis. The primary goal was to identify the most favorable conditions for nanoparticle production and durability, including concentration, temperature, and pH. The ultimate goal was to attain the highest level of inhibitory impact on these microorganisms.

This inquiry not only enhances the field of nano biotechnology but also fits with the worldwide effort to promote environmentally friendly and sustainable scientific procedures. This research enhances our comprehension of the biological production of nanoparticles and their interactions with microbial pathogens. Consequently, it opens up possibilities for novel applications in medicine, such as drug delivery systems and antimicrobial coatings. This has the potential to completely transform our methods of infection control and treatment [9, 10, and 11].

2. AIMS OF THE STUDY

Files must be in MS Word only and should be formatted for direct printing, using the CRC MS Word provided. Figures and tables should be embedded and not supplied separately.

Please make sure that you use as much as possible normal fonts in your documents. Special fonts, such as fonts used in the Far East (Japanese, Chinese, Korean, etc.) may cause problems during processing. To avoid unnecessary errors, you are strongly advised to use the ‘spellchecker’ function of MS Word. Follow this order when typing manuscripts: Title, Authors, Affiliations, Abstract, Keywords, Main text (including figures and tables), Acknowledgements, References, Appendix. Collate acknowledgments in a separate section at the end of the article and do not include them on the title page, as a footnote to the title or otherwise.

3. MATERIALS AND METHODS

3.1 Isolation and identification of E. coli

Subsequently, the homogenized samples were put into nutritional broth (NB, 5 mL per test tube, HiMedia) and cultured at 37°C for 24 hours to enhance their growth. A tiny portion of the inoculum from NB was then streaked in triplicate onto EMB agar plates and incubated at 37°C overnight, following the method described by the colonies with a metallic green gloss and dark centers .The isolated colonies underwent many sub-culturing procedures to evaluate the consistency of their appearance. It was possible to tell what kind of bacteria it was by looking at the colony's features, its shape using Gram's staining, the sugar fermentation test, and different biochemical tests like methyl red, Voges-Proskauer (V-P), catalase, and coagulase. The microorganisms were cultivated in nutrient broth media to produce biomass. The culture was grown on a rotary shaker at 100 revolutions per minute. Following 24 hours of cultivation, the biomass was collected by centrifugation at a speed of 12,000 revolutions per minute for 10 minutes. The liquid portion and solid residue were used to produce silver nanoparticles [12, 13, 14].

3.2 Identification of E. coli isolates using the analytical profile index (API) 20E.

The API 20E method for standardized identification was created by Biomerieux in France and is designed to find Enterobacteriaceae and other Gram-negative rods. It was used to identify E. coli. E. coli isolates were grown on EMB agar and incubated at a temperature of 37°C for a period of 18 to 24 hours. The identification test for E. coli isolates was performed in accordance with the manufacturer's instructions. To obtain a uniform bacterial solution for specific colonies, API 20E medium was used. The API 20E media was infected and used to fill both the tubes and cupules of the API 20E. To achieve anaerobiosis in the arginine dihydrolase, lysine decarboxylase, ornithine decarboxylase, urease, and H2S generation assays, the cupules were filled with sterile mineral oil to create a raised, curved surface. The incubation boxes were sealed and placed in an incubator set at a temperature of 37°C for a duration of 18 to 24 hours. Based on API 20E's numerical profile, isolate identification was conducted based on the numerical profile of API 20E [15, 16].

3.3 Green synthesis of AgNPs

AgNPs can be synthesized through biological means. The chosen bacterial strain was introduced into a 250-ml Erlenmeyer flask containing 100 ml of sterilized Tryptic Soy Broth (TSB). The flasks were placed in a shaking incubator and kept at a temperature of 37°C for a duration of 24 hours. The shaking speed was set at 120 revolutions per minute. Following incubation, the culture underwent centrifugation at a speed of 10,000 revolutions per minute for a duration of 10 minutes, resulting in the separation of the bacterial pellet. The liquid portion was combined with a sterilized solution of AgNO3 at a final concentration of 1 mM. The mixture was then placed in an orbital shaker and incubated at a temperature of 37°C while being agitated at a speed of 200 revolutions per minute. The extracellular production of AgNPs was evaluated by visually observing the color change in the culture medium. Following the incubation process, the mixture underwent centrifugation at 2000 rpm for 5 minutes to eliminate any leftover medium components. Subsequently, the AgNPs were gathered using high-speed centrifugation at 20,000 rpm for 10 minutes. The result was washed many times using centrifugation and then redisposed in water to eliminate any remaining

unconverted silver ions. Ultimately, the AgNPs were gathered into a compact mass and used for characterization [17, 18].

3.4 Characterization of Biosynthesized Silver Nanoparticles

Scanning Electron Microscopy (SEM)
Scanning electron microscopy was performed in order to determine the size and shape of AgNPs. A small amount of AgNPs sample was dropped on a carbon- coated copper, then left to dry for 5 minutes. After that, the sample was analyzed by SEM [19].

3.5 X-Ray Diffraction (XRD)

Crystalline structure of AgNPs was detected using X-ray diffraction technique. Slide was prepared from the purified powder of AgNPs and analyzed by XRD. The patterns of XRD were measured with Cu Kα radiation (λ=1.54 A) on 2θ angle in the range of 20 to 80 degrees. The Crystalline size of AgNPs was calculated using Scherrer equation: $D=k\lambda / \beta \cos\theta$ Where D: Average crystalline size K: Scherrer constant = 0.89 λ: X-ray wavelength = 1.5406 β: Full-Width half maximum (FWHM) = 0.52000 θ: Bragg angle = 38.164/2 [20].
Energy-dispersive X-ray (EDX) analysis
The Energy Dispersive X-ray (EDX) microanalysis is a technique of elemental analysis associated with electron microscopy based on the generation of characteristic Xrays that reveals the presence of elements present in the specimens [21]

3.6 Antibacterial activity of silver nanoparticles (AgNPs) in-vitro

The study of the antibacterial activity of the aqueous and alcoholic AgNPs against the antibiotic-resistant bacterial isolate was carried out by transferring 0.1 ml of standardized bacterial inoculum (1.5 ×105 CFU/ml, 0.5 McFarland's standard) and 0.1 ml of each concentration prepared from the aqueous and alcoholic AgNPs to the sterile test tube. After incubation at 37 °C for one hour, the mixture was poured onto sterile Mueller-Hinton agar plates (MHA) and spread by a spreader. All the plates were incubated at 37 °C for 24 hours. The antibacterial activity was observed by counting bacterial colonies and compared with the control. Three plates (replicates) were used for each concentration to reduce the errors that might result from conducting the experimenting [22].

4. Results and discussion

The antibacterial activity of nano-silver (Nano-AgNO3) against three bacterial strains, namely E. coli, S. aureus, and B. subtilis, is being investigated. The numbers show the size of the inhibition zone in millimeters for each type of bacteria when nano-AgNO3 was added in different amounts (20, 40, 60, 80, and 100 µg/mL). For all bacterial strains, the antimicrobial activity increased proportionally with the concentration of nano-AgNO3. This suggests that the effectiveness of nano-AgNO3 in killing bacteria is influenced by its concentration. The impact varies depending on the strain. The diameter of the inhibition zone varies across different bacterial strains. E. coli exhibits the greatest inhibitory zone diameter at all concentrations, with S. aureus and B. subtilis following suit. These findings indicate that E. coli is more vulnerable to nano-AgNO3 than S. aureus and B. subtilis. The effective concentration range for E. coli is 20–40 µg/mL, whereas for S. aureus it is 40–60 µg/mL, and for B. subtilis it is 60–80 µg/mL. Nano-AgNO3 nanoparticles can disrupt the cell membrane, causing injury and releasing cellular contents. This impedes the cell's ability to maintain its internal milieu, resulting in cellular death. Nano-AgNO3 can induce reactive oxygen species (ROS) production. These ROS include superoxide radicals and hydroxyl radicals, which possess high reactivity and have the potential to cause damage to biological components such as DNA, proteins, and lipids. Oxidative stress has the potential to finally result in cellular death. It is possible for nano-AgNO3 to bind to and stop the activity of important bacterial enzymes. This can mess up important metabolic processes and kill cells. The variations in susceptibility among the bacterial strains may be attributed to variances in their cell wall construction, membrane composition, and enzyme activity. Nano-AgNO3 ability to kill bacteria can also be affected by things like the size and shape of the nanoparticles, as well as the presence of other ions in the solution.

Table 1: Inhibition Zone Diameters of Different Bacteria in Response to Nano Silver Concentrations

Bacteria	Inhibition zoon diameter of Nano Silver (Nano-AgNO3)				
	20 µg/mL	40 g/mL	60 µg/mL	80 µg/mL	100 µg/mL
E coli	10	13	15	16	19
S. aureus	9	12	14	17	20
B. subtilis	9	9	12	16	18

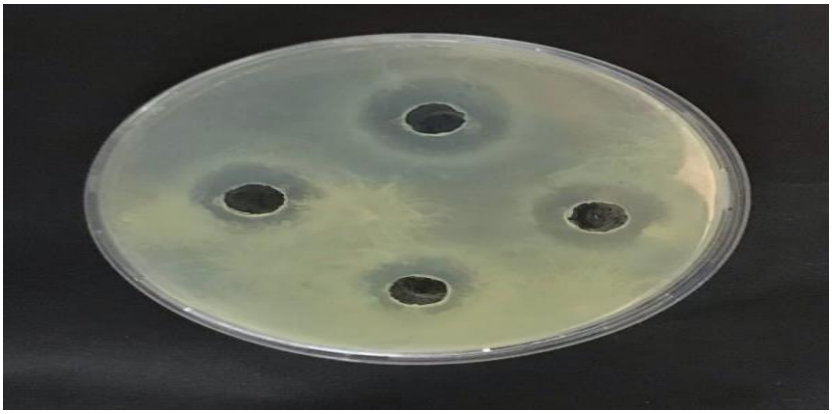

Figure1: Antimicrobial Susceptibility Testing on Agar Plate

The anti-bacterial action is size-dependent for nanoparticles, with smaller nanoparticles having a greater surface area in contact with bacterial cells and a higher ability to enter the cytoplasm compared to larger nanoparticles [28]. The cell membrane of bacteria carries a negative charge as a result of the presence of carboxyl and phosphate groups, as well as amino groups [29]. Hence, the silver nanoparticles possess a positive charge that enables them to attract the negatively charged cell membrane, thereby facilitating the attachment of the AgNPs to the membranes of bacterial cells [30]. Silver nanoparticles can penetrate the bacterial cell through the cell membrane and engage with various structures and essential molecules such as proteins, lipids, and amino acids. This interaction between AgNPs and cellular structures or biomolecules results in their malfunction and demise. Ultimately, bacteria. Specifically, the contact between AgNPs and ribosomes results in their denaturation, causing the suppression of translation and protein production. In addition, the antibacterial function of AgNPs is attributed to their capacity to generate substantial quantities of reactive oxygen species (ROS), including hydrogen peroxide, oxygen radicals, and singlet oxygen [31].

Table2:

Bacteria	Source of Variation	Sum of Squares (SS)	Degrees of Freedom (df)	Mean Square (MS)	F-Value	P-Value
E. coli	**Between Groups**	84.8	4	21.2	14.13	0.0067
	Within Groups	6.0	5	1.2		
	Total	90.8	9			
S. aureus	**Between Groups**	91.6	4	22.9	19.08	0.0033
	Within Groups	6.0	5	1.2		
	Total	97.6	9			
B. subtilis	**Between Groups**	88.8	4	22.2	10.32	0.0137
	Within Groups	10.8	5	2.16		
	Total	99.6	9			

ANOVA Results for Variability in Response to Treatment among Bacteria

Furthermore, figure (2) displays the outcomes of an API 20 E test, which is a diagnostic instrument utilized to identify gram-negative bacteria by analyzing their biochemical characteristics. The bacterium tested has been identified as Escherichia coli with a confidence level of 92.6%, based on the profile number "1 4 4 4 5 2 5 7". This profile indicates a distinct pattern of metabolic activity that is characteristic of E. coli. The 'T' value of 0.54 suggests that the test findings are relatively representative of E. coli. Another potential identification is Citrobacter freundii, although the level of certainty is far lower at only 4.0%, which makes it improbable. The test results indicate a significant presence of hydrogen sulfide generation, a rather uncommon trait in E. coli, found in only 1% of strains. This extensive biochemical profiling offers a dependable approach to identifying the bacterial species, with E. coli being the most probable bacterium in this particular situation.

(a)

(b)

GOOD IDENTIFICATION	
Strip	API 20 E V5.0
Profile	1 4 4 4 5 5 2 5 7
Note	

Significant taxa	% ID	T	Tests against					
Escherichia coli 1	92.6	0.54	H2S	1%				

Next taxon	% ID	T	Tests against					
Citrobacter freundii	4.0	0.31	CIT	75%	IND	1%	SAC	99%

Figure2: API 20 E Biochemical Test Results for Bacterial Identification

A detailed X-ray diffraction (XRD) analysis of the material's crystallographic characteristics is included in the data. Detected peaks at 2θ points indicate crystallographic planes, crucial for establishing crystal structure, lattice parameters, and other properties. Peak 1 is located at 27.0749° 2θ with a d-spacing of 3.29074 Å. It has a modest intensity and a wider FWHM of 1.0084°. This suggests smaller crystallite sizes (about 46 Å) and a higher microstrain (3.61379%). These crystallites have substantial lattice aberrations or defects. Internal stresses may affect the material's mechanical qualities or reactivity. Peak 2 is the most intense and dominates the spectra, positioned at 31.4531° 2θ with a d-spacing of 2.84194 Å. This peak shows that Peak 2 is the crystallite orientation. The peak sharpness and narrow FWHM value of 0.1573° suggest bigger crystallite sizes (approximately 700 Å) with a minimum microstrain of 0.2031%. The crystal structure seems homogeneous and defect-free, indicating good stability and material strength.

However, Peak 3 at 37.8347° 2θ is well-defined and has a modest microstrain of 0.00403%. Its intensity is surprisingly low. This could be an experimental error or instrumental abnormality that needs more investigation. Peaks 4-7 show varying crystallite strengths and sizes, from 473 Å to 640 Å. These peaks have modest microstrains of 0.09873% to 0.21182%. Materials with multiple crystal structures have these peaks, which represent crystal quality and alignment variance. This variance may affect the material's physical and chemical properties in various applications. XRD tests highlight the primary crystal orientations and changes in crystallite size and strain in different planes, revealing the material's crystallinity. This knowledge is crucial for understanding the material's prospective uses and performance in numerous industrial and technological domains, especially when exact crystalline properties are needed. [27] Reported that the scattering XRD spectrum of silver nanoparticles showed four peaks at Bragg's angles which conformed to the metallic silver phase (JCPDS file no. 04-0783). They were related to crystalline planes (111), (200), (220), and (311), and the intensity of peaks for plane (111) was stronger. Peaks arising from 2θ at 38, 34, 64, and 77 were crystalline planes of (111), (200), (220), and (311), respectively. These peaks caused by Bragg scattering indicate the formation of crystalline silver nanoparticles with spiral structure and an A equal to 4.086

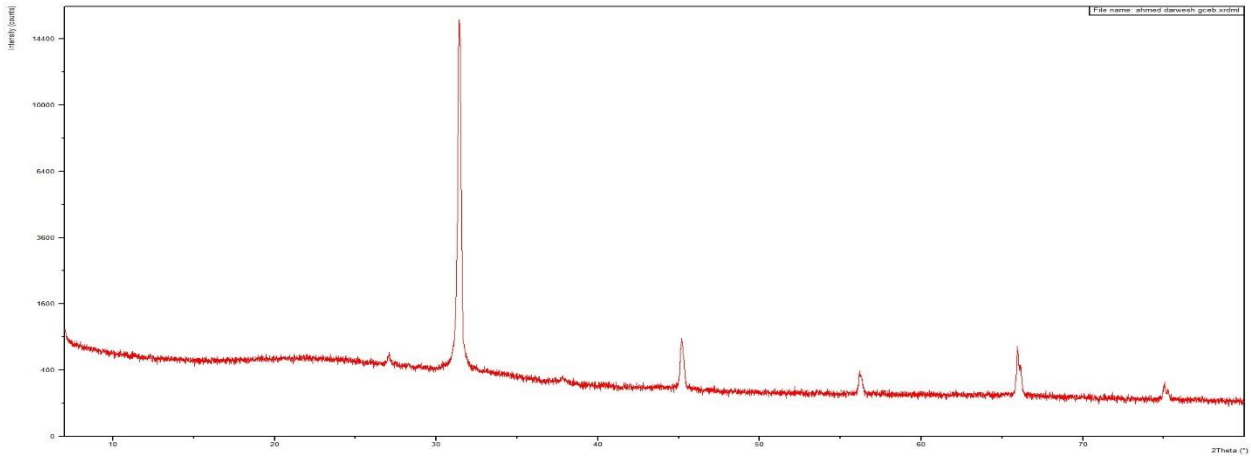

Figure3: XRD Pattern of Crystalline Material.

Most nanoparticles are spherical but vary in form and size. Diameters from 66.99 to 119.2 nm demonstrate moderate to outstanding monodispersity. This is necessary for a uniform application. Certain photos reveal nanoparticle clustering, which may impact surface area, reactivity, and properties. High-resolution photos show that nanoparticles' flat surface helps medication delivery systems with less biological contact. Distribution: Nanoparticles are uniformly scattered, but they cluster in the magnification photos. Agglomeration can be affected by synthesis or post-synthesis drying. Agglomeration affects nanoparticle surface area, catalysis, and antibacterial activity. Nanoparticle size and surface reveal high antibacterial capabilities. Reduced nanoparticles can better penetrate bacterial cell membranes, disrupting biology. Increased size and shape uniformity in the synthesis process may indicate improved consistency. This is crucial for industrial reproduction accuracy. Size and surface qualities allow us to design nanoparticles for targeted medicine, wound healing, electronics, and catalysis. Similar to a study by [23] that discovered , silver nanoparticles had a rate of 42 nm. As in study [24], the rate of AgNPs was determined. 43nm. 65.33 nm, 43.82 nm, [25] reported that SEM images of silver nanoparticles were of spherical shape and appeared to be reasonably monodispersed. The sizes of the silver particles were found to be in the range of 5–25 nm diameter. [26] Reported biosynthesis of silver nanoparticles using culture supernatant of newly isolated Bacillus sp. Monodispersed silver nanoparticles in the range of 50 to 120 nm were synthesised extracellularly. Such variation in shape and size for nanoparticles synthesized by biological systems is commonly obtained. However, if the process of silver nanoparticles is to be a viable alternative to the current chemical method, then greater control over particle size and polydispersity would be required [26].

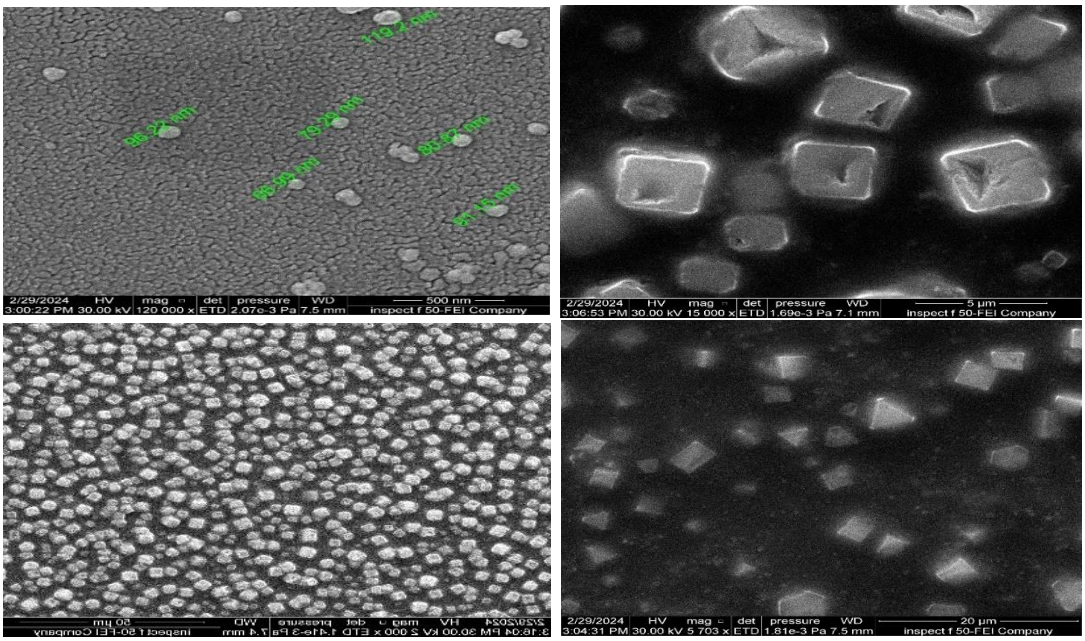

Figure 4: Silver Nitrate Nanoparticles under SEM in Different Scales

The chemical composition of the produced samples was assessed by determining their elemental makeup using EDX, a diagnostic tool. Silver nanoparticles' EDX spectra are shown in Figure (4). Peaks corresponding to the presence of oxygen and silver suggested the formation of a silver complex. Two separate reports are generated from the data, each offering an elemental analysis of the two locations. Using two EDx, the composition is detected using energy-dispersive X-ray spectroscopy. Carbon (C), oxygen (O), and silver (Ag) are consistently mentioned in all reports, suggesting that they are frequent elements. The investigations also show that other elements, such as sodium (Na), magnesium (Mg), silicon (Si), chlorine (Cl), and calcium (Ca), are present in varying quantities. This could be due to differences in the surrounding environment or the composition of the samples taken from each site. The presence of organic substances or significant oxidation reactions is implied by the higher carbon and oxygen levels observed in all reports. Discrepancies in reported percentages among papers may be due to inherent sample variability, differences in data processing, or exposure to different situations. Silver was found in all the reports, though in different concentrations. The nanoparticles being studied contain silver, which is a very important element. Varying nanoparticle concentrations may be an indication of dispersion, aggregation, or degradation as a result of exposure to environmental factors. In addition, these differences could be caused by particular features at various locations.

There was a wide variety of components at the first site, including large amounts of NA, CL, and Si. This finding raises the possibility of being exposed to environments that are rich in silicon or salt. In the next spot, the secondary components showed less variation, but the primary ones (C, X, and AG) were always there. Important information on the chemical make-up of the samples under consideration was revealed by the ratios in the second place. The study uncovered three important features using 145,979 readings collected at an average rate of 4,784 readings per second for 32 seconds with an acceleration force of 30 KV. The majority of the composition is oxygen, which makes up 57.7% (± 1.2%) by atomic number and 54.5% (± 1.1%) by weight. Carbon is 39.6% (± 1.2%) heavy and 28.1% (± 0.8%) atomic by mass. Based on atomic number, 2.7% (±0.1%) of the composition is silver, while based on weight, 17.4% (±0.6%) is silver. It denotes a less susceptible or more regulated environment. There seems to be some variance in the sample or possible contamination, since P and K appear together in one report and MG in another. We are tracking the time of data collection and the frequency of occurrences using different approaches and increasing the frequency of data collection. When discussing factors that affect the detection of X-ray emissions, the emphasis is on changes in sample density, thickness, or initial composition. Reliability of the measurements is supported by the small errors in atomic weight and proportions. However, variations in error rates may also indicate varying levels of certainty in the initial quantitative measurement, which could be affected by the samples' physical state or composition.

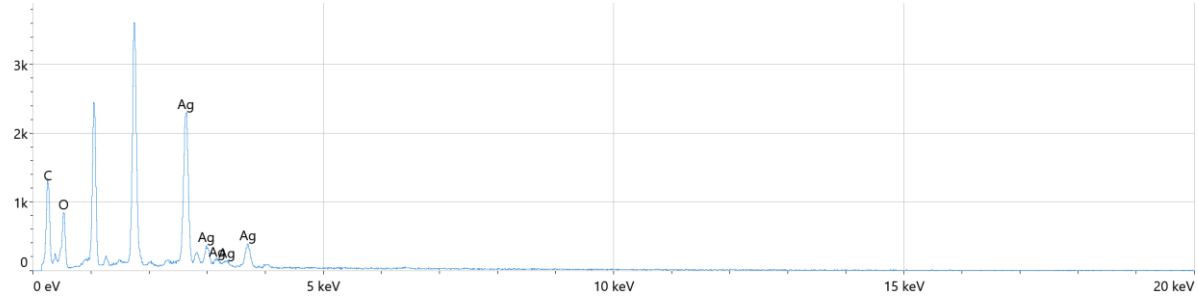

Figure5: Energy Dispersive X-ray (EDX) Spectrum of Silver Nanoparticles

Table 3: Elemental Composition of the Sample by EDX Analysis

Element	Atomic %	Atomic % Error	Weight %	Weight % Error
C	35.0	1.3	23.3	0.8
O	61.2	1.2	54.2	1.1
Ag	3.8	0.1	22.6	0.7

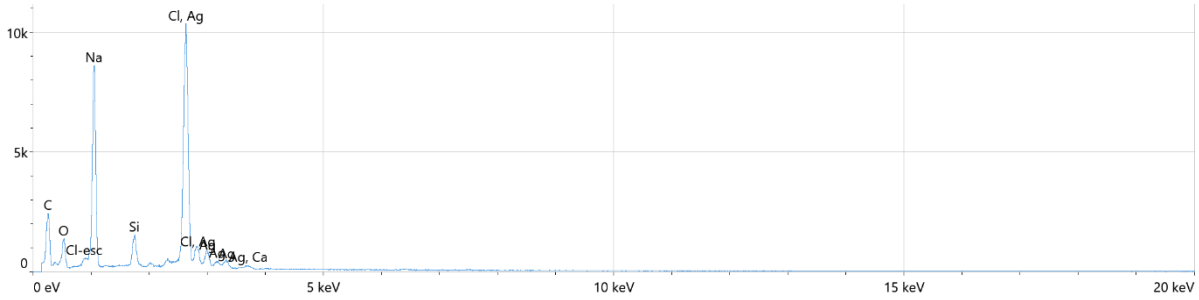

Figure 6: EDS Spectrum of a Multi-Element Sample

Table4: Elemental Composition and Error Analysis of a Sample

Element	Atomic %	Atomic % Error	Weight %	Weight % Error
C	54.4	0.6	36.6	0.4
O	16.0	0.3	14.4	0.3
Na	17.2	0.1	22.2	0.1
Si	1.5	0.0	2.4	0.0
Cl	9.9	0.1	19.7	0.1
Ca	0.3	0.0	0.6	0.0
Ag	0.7	0.0	4.1	0.1

5. CONCLUSION

Green synthesis of AgNPs using E. coli is an efficient and environmentally friendly way to make antimicrobial nanoparticles. Escherichia coli, Staphylococcus aureus, and Bacillus subtilis were strongly inhibited by AgNPs at higher concentrations. EDX, XRD, and SEM studies validated the nanoparticles' structural properties and production. This research advances nanotechnology and ecologically sustainable scientific methods worldwide. The data suggest that AgNPs may treat bacterial infections, especially those resistant to conventional antibiotics. This discovery could improve healthcare and medicine. Future research may focus on improving nanoparticle synthesis to increase yield and efficacy and explore their biomedical applications.

REFERENCES

[1] R. Ahmad, N. Aramesh, S. Hasnain, A. K. Nayak, and R. Varma, "Greener fabrication of metal nanoparticles using plant materials: A review," Chemical Physics Impact, vol. 2023, Art. no. 100255, 2023, doi: 10.1016/j.chphi.2023.100255.
[2] R. Bishwas, S. Jahan, and M. A. Alam, "An Investigation on Synthesis of Silver Nanoparticles," Asian Journal of Research in Biochemistry, vol. 12, pp. 1-10, 2023, doi: 10.9734/ajrb/2023/v12i3234.
[3] W. Zhang, G. Ye, D. Liao, X. Chen, C. Lu, A. Nezamzadeh-Ejhieh, M. S. Khan, J. Liu, Y. Pan, and Z. R. Dai, "Recent Advances of Silver-Based Coordination Polymers on Antibacterial Applications," Molecules, vol. 27, no. 27, Art. no. 2717166, 2022, doi: 10.3390/molecules27217166.
[4] A. J. Jasem and M. A. Mahmood, "Preparation and Characterization of Amoxicillin-loaded Chitosan Nanoparticles to Enhance Antibacterial Activity against Dental Decay Pathogens," Journal of Emergency Medicine, Trauma & Acute Care, vol. 3, Art. no. 10, 2023, https://doi.org/10.5339/jemtac.2023.midc.10.
[5] R. Devadharshini, G. Karpagam, K. Pavithra, S. Kowsalya, P. P. Mohana, and R. Mohanram, "Green Synthesis of Silver Nanoparticles," Microbiology Research Journal International, vol. 33, pp. 1-9, 2023, doi: 10.9734/mrji/2023/v33i51380.
[6] V. Maharani, A. Sundaramanickam, and T. Balasubramanian, "In vitro anticancer activity of silver nanoparticle synthesized by Escherichia coli VM1 isolated from marine sediments of Ennore southeast coast of India," Enzyme Microb Technol., vol. 95, pp. 146-154, Dec. 2016, doi: 10.1016/j.enzmictec.2016.09.008.
[7] Dr. M. Ramaiah, S. Ignacimuthu, a. J. a. Ranjitsingh, R. Krishnamoorthy, and M. Paulraj, "Culture Method-Dependent Variation in the Sensitivity of Escherichia coli to Silver Nanoparticles," Advances in Materials Science and Engineering, vol. 2023, pp. 1-6, 2023, doi: 10.1155/2023/1680311.
[8] O. Daramola, N. Torimiro, and S. Alayande, "Affinity capture of Escherichia coli pathotypes using poly-L-lysine functionalized silver nanoparticles," Advances in Natural Sciences: Nanoscience and Nanotechnology, vol. 13, Art. no. 025012, 2022, doi: 10.1088/2043-6262/ac7712.
[9] B. Essghaier, H. Hannachi, R. Nouir, F. Mottola, and L. Rocco, "Green Synthesis and Characterization of Novel Silver Nanoparticles Using Achillea maritima subsp. maritima Aqueous Extract: Antioxidant and Antidiabetic Potential and Effect on Virulence Mechanisms of Bacterial and Fungal Pathogens," Nanomaterials (Basel), vol. 13, no. 13, Art. no. 1964, Jun. 28, 2023, doi: 10.3390/nano13131964

[10] N. González-Ballesteros, M. Fernandes, R. Machado, P. Sampaio, A. C. Gomes, A. Cavazza, F. Bigi, and M. C. Rodríguez-Argüelles, "Valorisation of the Invasive Macroalgae Undaria pinnatifida (Harvey) Suringar for the Green Synthesis of Gold and Silver Nanoparticles with Antimicrobial and Antioxidant Potential," Marine Drugs, vol. 2023, doi: 10.3390/md21070397, 2023.
[11] K. Rajak, P. Pahilani, H. Patel, B. Kikani, R. Desai, and H. Kumar, "Green synthesis of silver nanoparticles using Curcuma longa flower extract and antibacterial activity
[12] F. A. Ema, R. N. Shanta, M. Z. Rahman, M. A. Islam, and M. M. Khatun, "Isolation, identification, and antibiogram studies of Escherichia coli from ready-to-eat foods in Mymensingh, Bangladesh," Vet World, vol. 15, no. 6, pp. 1497-1505, Jun. 2022, doi: 10.14202/vetworld.2022.1497-1505.
[13] M. Cheesbrough, Medical Laboratory Manual for Tropical Countries, 1st ed., English Language Book Society, London, pp. 400-480, 1985.
[14] M. Cheesbrough, District Laboratory Practice in Tropical Countries, 2nd ed., Cambridge University Press, Cambridge, UK, 2006.
[15] T. Ramatla, "The Utility of MALDI-TOF-Mass Spectrometry, Analytical Profile Index (API) and Conventional-PCR for the Detection of Foodborne Pathogens from Meat," Journal of Food and Nutrition Research, vol. 9, doi: 10.12691/jfnr-9-8-7, 2021.
[16] F. Mohamed et al., "Iodometric and Molecular Detection of ESBL Production Among Clinical Isolates of E. coli Fingerprinted by ERIC-PCR: The First Egyptian Report Declares the Emergence of E. coli O25b-ST131clone Harboring blaGES," Microbial Drug Resistance, doi: 10.1089/MDR.2016.0181, 2017.
[17] R. Devadharshini, G. Karpagam, K. S. Pavithra, S. Kowsalya, P. Mohana Priya, and A. Ramachandran, "Green Synthesis of Silver Nanoparticles," Microbiology Research Journal International, doi: 10.9734/mrji/2023/v33i51380, 2023.
[18] D. K. Divya, L. C. Kurian, S. Vijayan, and M. S. Jisha, "Green synthesis of silver nanoparticles by Escherichia coli: Analysis of antibacterial activity," J. Water Environ. Nanotechnol., vol. 1, no. 1, pp. 63-74, doi: 10.7508/jwent.2016.01.008, 2016.
[19] S. Muthukrishnan, S. Bhakya, T. S. Kumar, and M. V. Rao, "Biosynthesis, characterization and antibacterial effect of plant-mediated silver nanoparticles using Ceropegia thwaitesii–An endemic species," Industrial Crops and Products, vol. 63, pp. 119-124, 2014.

[20] S. Vanaraj, B. B. Keerthana, and K. Preethi, "Biosynthesis, characterization of silver nanoparticles using quercetin from Clitoria ternatea L to enhance toxicity against bacterial biofilm," Journal of Inorganic and Organometallic Polymers and Materials, vol. 27, no. 5, pp. 1412-1422, 2017.
[21] G. H. Vale De Macedo et al., "Interplay between ESKAPE Pathogens and Immunity in Skin Infections: An Overview of the," [Journal Name], [Volume], [Page Numbers], [Year]. Note: Complete publication details needed.
[22] M. Balouiri, M. Sadiki, and S. K. Ibnsouda, "Methods for in vitro evaluating antimicrobial activity: A review," Journal of Pharmaceutical Analysis, vol. 6, pp. 71-79, 2016.
[23] P. Ghorbani et al., "Sumac silver novel biodegradable nanocomposite for biomedical application: Antibacterial activity," Molecules, vol. 20, pp. 12946-12958, 2015, doi: 10.3390/molecules20117272
[24] B. Das, S. K. Dash, D. Mandal, T. Ghosh, S. Chattopadhyay, S. Tripathy, S. Das, S. K. Dey, D. Das, and S. Roy, "Green synthesized silver nanoparticles destroy multidrug- resistant bacteria via reactive oxygen species mediated membrane damage," Arabian Journal of Chemistry, vol. 10, pp. 862-876, 2017, doi: 10.1016/j.arabjc.2015.06.023.
[25] A. E.-R. R. El-Shanshoury, S. E. ElSilk, and M. E. Ebeid, "Extracellular biosynthesis of silver nanoparticles using Escherichia coli ATCC 8739, Bacillus subtilis ATCC 6633, and Streptococcus thermophilus ESh1 and their antimicrobial activities," ISRN Nanotechnology, vol. 2011, Art. no. 2011, 2011, doi: 10.5402/2011/825430.
[26] M. Kowshik, et al., "Extracellular synthesis of silver nanoparticles by a silver-tolerant yeast strain MKY3," Nanotechnology, vol. 14, no. 1, p. 95, 2003, doi: 10.1088/0957-4484/14/1/321.
[27] M. Gholami-Shabani, et al., "Antimicrobial Activity and Physical Characterization of Silver Nanoparticles Green Synthesized Using Nitrate Reductase from Fusarium oxysporum," Applied Biochemistry and Biotechnology, vol. 172, no. 8, pp. 4084-4098, 2014, doi: 10.1007/s12010-014-0856-2.
[28] M. Seong and D. G. Lee, "Silver nanoparticles against Salmonella enterica serotype Typhimurium: role of inner membrane dysfunction," Current Microbiology, vol. 74, pp. 661-670, 2017, doi: 10.1007/s00284-017-1198-4.
[29] A. Van Der Wal, W. Norde, A. J. B. Zehnder, and J. Lyklema, "Determination of the total charge in the cell walls of Gram-positive bacteria," Colloids and Surfaces B: Biointerfaces, vol. 9, pp. 81-100, 1997, doi: 10.1016/S0927-7765(96)01342-0.
[30] A. Abbaszadegan, Y. Ghahramani, A. Gholami, B. Hemmateenejad, S. Dorostkar, M. Nabavizadeh, and H. Sharghi, "The Effect of Charge at the Surface of Silver Nanoparticles on Antimicrobial Activity against Gram-Positive and Gram Negative Bacteria: A Preliminary Study," Journal of Nanomaterials, vol. 2015, Art. no. 720654, 2015, doi: 10.1155/2015/720654.
[31] Masadeh MM, Al-Tal Z, Khanfar MS, Alzoubi KH, Sabi SH, Massadeh MM. Synergistic Effect of Silver Nanoparticles with Antibiotics for Eradication of Pathogenic Biofilms. Curr Pharm Biotechnol. 2024 Jan 12. doi: 10.2174/0113892010279217240102100405. Epub ahead of print. PMID: 38231054.